The Journal of Experimental Biology 215, 2039-2050

doi:10.1242/jeb.065094

RESEARCH ARTICLE

Mitochondrial function in sparrow pectoralis muscle

Sarah Kuzmiak, Brian Glancy, Karen L. Sweazea and Wayne T. Willis*

Arizona State University, Department of Kinesiology, Tempe, AZ 85287, USA

*Author for correspondence (waynewillis@asu.edu)

SUMMARY

Flying birds couple a high daily energy turnover with double-digit millimolar blood glucose concentrations and insulin resistance. Unlike mammalian muscle, flight muscle predominantly relies on lipid oxidation during locomotion at high fractions of aerobic capacity, and birds outlive mammals of similar body mass by a factor of three or more. Despite these intriguing functional differences, few data are available comparing fuel oxidation and free radical production in avian and mammalian skeletal muscle mitochondria. Thus we isolated mitochondria from English sparrow pectoralis and rat mixed hindlimb muscles. Maximal O_2 consumption and net H_2O_2 release were measured in the presence of several oxidative substrate combinations. Additionally, NAD- and FAD-linked electron transport chain (ETC) capacity was examined in sonicated mitochondria. Sparrow mitochondria oxidized palmitoyl-L-carnitine 1.9-fold faster than rat mitochondria and could not oxidize glycerol-3-phosphate, while both species oxidized pyruvate, glutamate and malate–aspartate shuttle substrates at similar rates. Net H_2O_2 release was not significantly different between species and was highest when glycolytic substrates were oxidized. Sonicated sparrow mitochondria oxidized NADH and succinate over 1.8 times faster than rat mitochondria. The high ETC catalytic potential relative to matrix substrate dehydrogenases in sparrow mitochondria suggests a lower matrix redox potential is necessary to drive a given O_2 consumption rate. This may contribute to preferential reliance on lipid oxidation, which may result in lower *in vivo* reactive oxygen species production in birds compared with mammals.

Key words: skeletal muscle mitochondria, substrate oxidation, aging, reactive oxygen species, bird.

Received 21 September 2011; Accepted 22 February 2012

INTRODUCTION

Flying birds couple a long lifespan with a high metabolic rate, as well as a chronically high blood glucose concentration (~15 mmol l^{-1}) and insulin resistance (Belo et al., 1976; Gee et al., 1981; Sweazea and Braun, 2005). The fact that birds live three to four times longer than mammals of similar body mass and have higher resting metabolic rates (RMRs) (Calder, 1996; Holmes and Austad, 1995) argues against the dependence of longevity on the rate of living, i.e. the life energy potential concept of Pearl (Pearl, 1928). Harman's alternative free radical theory of aging (Harman, 1956), that the rate of senescence primarily depends on the rate of free radical production, is supported by data showing that caloric restriction in rats decreases mitochondrial reactive oxygen species (ROS) production (Masoro, 1992; Sohal et al., 1994) and increases lifespan without affecting RMR (McCarter et al., 1985; McCarter and McGee, 1989). Harman's concept is also consistent with many avian *vs* mammalian comparative studies measuring ROS production by mitochondria isolated from a number of tissues and species. Herrero and Barja found that the rate of pyruvate + malate (P+M)-supported ROS production was greater in rat compared with pigeon in both heart and nonsynaptic brain mitochondria (Barja, 1998; Barja and Herrero, 1998; Herrero and Barja, 1997), and also in mouse compared with parakeet and canary heart mitochondria (Herrero and Barja, 1998). Ku and Sohal found lower free radical production in pigeon compared with rat brain, heart and kidney mitochondria oxidizing the unphysiological substrate succinate (Ku and Sohal, 1993), whereas another investigation by Brown et al. found that free radical production was higher in sparrow *vs* mouse liver mitochondria with either succinate or glutamate + malate as substrates (Brown et al., 2009). These investigations utilized an assortment of different conditions to make their assessments and examined limited substrate combinations, producing varied results in both direction and magnitude.

Increased antioxidant capacity in avian compared with mammalian species may result in lower overall ROS damage, as cellular ROS is a function of the rate of ROS production and the rate of ROS scavenging. However, investigations into the antioxidant capacity of these species have yielded conflicting results. Ku and Sohal found higher superoxide dismutase and glutathione peroxidase levels in pigeon compared with rat tissues, but a lower level of catalase (Ku and Sohal, 1993). Perez-Campo reported a negative correlation between lung glutathione reductase activity and maximum lifespan in birds and mammals (Perez-Campo et al., 1993), which agrees with the findings by Barja et al. of lower antioxidant capacity in pigeon than rat brain, liver and lung (Barja et al., 1994). Taken together, these data indicate no clear correlation between antioxidant capacity and longevity.

The matrix oxidation/reduction (redox) potential strongly influences mitochondrial ROS production (Starkov and Fiskum, 2003). Pigeon pectoralis mitochondria possess high catalytic potential in the electron transport chain (ETC) relative to the entire oxidative pathway compared with mammalian muscle mitochondria (Rasmussen et al., 2004), which suggests that lower ROS production may be due, in part, to lower matrix redox pressure at a given substrate oxidation rate. On the basis of these previous observations, we hypothesized that high ETC maximum velocity (V_{max}) relative

to complete substrate oxidation pathways would be coupled with lower superoxide production (measured as net H_2O_2 release) in mitochondria from English sparrow (*Passer domesticus*) pectoralis compared with rat (*Rattus norvegicus*) mixed hindlimb muscle. Thus, one purpose of the present study was to measure the maximum (state 3) mitochondrial O_2 consumption rate ($\dot{J}_{O_2}$), ETC flux capacity in sonicated mitochondria from three sites of electron entry, and ROS production by intact 'resting' (oligomycin-inhibited) mitochondria. To our knowledge, no investigation into ROS production from avian muscle mitochondria currently exists.

Fuel selection by contracting muscles during locomotion differs markedly between birds and mammals. Humans and rats run at ~75% of their maximum rate of O_2 uptake ($\dot{V}_{O_2,max}$) with a respiratory quotient (RQ) at or above 0.90 (Brooks and Donovan, 1983; Brooks and Gaesser, 1980; O'Brien et al., 1993), which reflects a general pattern of carbohydrate dependence in mammals exercising at or above moderate intensity (Roberts et al., 1996). In contrast, pigeons fly at this intensity with an RQ of 0.73 (Rothe, 1987), indicating that pigeon flight muscle supports locomotion with the almost exclusive oxidation of fat. Additionally, calculated estimates of the migratory energy requirements of red knots, which are shorebirds, indicate that fat provides 95% of the fuel supply during flight (Jenni and Jennie-Eiermann, 1998). Although pigeons exhibit minimal changes in blood glucose concentrations during flights lasting 2–10 h (Bordel and Haase, 1993; Schwilch et al., 1996), mammalian dependence on carbohydrates at a similar relative intensity depletes body carbohydrate stores and precipitates fatigue, which coincides with low muscle glycogen and blood glucose (Ahlborg et al., 1974; Baldwin et al., 1973; Coyle, 1995; Fitts et al., 1975; Holloszy and Coyle, 1984; Wahren et al., 1971).

Both training and diet have been shown to modulate fuel selection; however, these effects are modest compared with the apparent differences that exist between avians and mammals. At a given absolute workload, trained individuals exhibit lower respiratory exchange ratio (RER) values compared with untrained individuals; however, when matched for % $\dot{V}_{O_2,max}$, the RER does not appear to be different during moderate and moderate–high intensity exercise (Bergman and Brooks, 1999; Hurley et al., 1986). Indeed, both absolute and relative fatty acid oxidation were the same in trained and untrained cyclists (Bergman and Brooks, 1999). Additionally, Roberts et al. demonstrated that dogs and goats have identical RER values at a given relative intensity, despite a twofold greater $\dot{V}_{O_2,max}$ in the dog (Roberts et al., 1996). In terms of the effect of diet, Heldge et al. found that a high-fat diet resulted in a decrease in leg RQ from 0.91 to 0.87 during minutes 30–60 of cycling exercise at 68% $\dot{V}_{O_2,max}$, with no effect during the first 30 min (Helge et al., 2001), whereas Burke et al. found that a high-fat diet decreased RER from 0.95 to 0.91 during minutes 20–40 of cycling exercise at 70% $\dot{V}_{O_2,max}$, with no differences seen from 40 to 120 min (Burke et al., 2002). Based on these data, during the intervals where fuel oxidation differed between control and high-fat diet groups, the fraction of energy coming from fat increased by ~62%, compared with a 170% increase when comparing rats with pigeons (Brooks and Donovan, 1983; Burke et al., 2002; Helge et al., 2001; Rothe et al., 1987). These data indicate that although diet can slightly modulate the amount of fat oxidized to fuel exercise, the changes are relatively small and may only occur at certain intensities or intervals.

Mammalian preference for carbohydrate fuel is also observed in mitochondria isolated from skeletal muscle, i.e. state 3 $\dot{J}_{O_2}$ is much higher with P+M than with palmitoyl-L-carnitine + malate (PC+M) (Baldwin et al., 1972; Davies et al., 1981; Jackman and Willis, 1996; Willis and Jackman, 1994). In hummingbird and pigeon pectoralis pyruvate and palmitate (both with added malate), state 3 rates are similar (Rasmussen et al., 2004; Suarez et al., 1991), but the fuel preferences of avian flight muscle mitochondria generally are unknown. Indeed, the ability to oxidize fatty acids to fuel flight would be necessary as the energy density of fatty acids is approximately eight times greater than stored glycogen (Flatt, 1995). Avian species, especially those that migrate, simply cannot afford to store fuel as carbohydrate. Thus, a second purpose of this study was to compare the oxidation rates of several physiological fuel combinations in sparrow pectoralis and rat hindlimb muscle mitochondria.

In mammalian skeletal muscle, increasing the rates of mitochondrial ATP production and O_2 consumption requires a rise in the cytosolic free ADP concentration ($[ADP]_f$) and a corresponding decline (less negative) in ATP free energy (ΔG_{ATP}) (Connett and Honig, 1989; Gyulai et al., 1985; Jeneson et al., 1995; Kushmerick et al., 1992). The ΔG_{ATP}:$\dot{J}_{O_2}$ relationship is near linear (Connett and Honig, 1989; Kushmerick et al., 1992). Kinetic control of $\dot{J}_{O_2}$ by $[ADP]_f$ alone (K_MADP), provides a nearly adequate transfer function (Kushmerick et al., 1992), although the relationship may be higher order (Jeneson et al., 1995). Isolated skeletal muscle mitochondria conform to these same relationships both in pattern and magnitude (Davis and Davis-Van Thienen, 1989; Glancy et al., 2008; Rottenberg, 1973). The sensitivity of mitochondria to kinetic signals such as $[ADP]_f$ and thermodynamic variables such as ΔG_{ATP} critically impacts both contractile performance and fuel selection because the declining muscle energy state both inhibits ATP utilization (Jeneson et al., 2000; Van der Meer et al., 1980) and activates the glycolytic pathway (Connett, 1988; Holloszy and Coyle, 1984; Saltin and Gollnick, 1983). It is therefore noteworthy that no data on the sensitivity of avian muscle mitochondria to respiratory signals currently exist. Thus, a third purpose of the present study was to evaluate K_MADP and the ΔG_{ATP}:$\dot{J}_{O_2}$ relationship ('force–flow' relationship or elasticity of mitochondrial $\dot{J}_{O_2}$ to extramitochondrial ATP free energy) in both rat and sparrow muscle mitochondria. Moreover, these kinetic parameters would be assessed with both carbohydrate (P+M) and fatty acid (PC+M) fuels.

Our results show that PC+M and P+M state 3 oxidation rates were closely matched in avian muscle mitochondria, in contrast to rodent muscle. The K_MADP for respiration was appreciably lower when mitochondria oxidized PC+M compared with P+M in both species, and the higher PC+M state 3 $\dot{J}_{O_2}$ in sparrow was consistent with a greater reliance on fatty acid fuel in avian mitochondria. The ETC relative capacity was markedly higher in bird muscle, but ROS production rates were generally similar. Moreover, in both sparrow and rat, ROS production was much higher for substrates related to aerobic glycolysis. The results suggest that avian dependence on lipid oxidation *in vivo* may result in lower ROS production compared with carbohydrate-dependent mammals.

MATERIALS AND METHODS

Mammalian and avian model species

An extensive body of literature supports the contention that the fuel mixture oxidized by a rat is representative of mammalian patterns in general, particularly in response to alterations in dietary macronutrient composition, metabolic rate due to exercise stress and skeletal muscle oxidative capacity elicited by training. Rat hindlimb also provides an abundant mass of type II muscle (the cell type accounting for most of avian flight muscle mass), yielding adequate mitochondrial protein to perform the mammalian experiments in

these studies. The choice of avian species was less clear. All published data indicate that fatty acid oxidation powers avian flight, with the exception of hovering hummingbirds in the act of ingesting carbohydrate (Suarez et al., 1990). We chose the English sparrow because our elucidation of mitochondrial metabolism would complement the work of Sweazea and Braun on glucose and fatty acid uptake by sparrow muscle (Sweazea and Braun, 2005; Sweazea and Braun, 2006). Additionally, this species is non-migratory in the southwestern United States (Anderson, 2006; Waddington and Cockrem, 1987). Finally, the data of Rasmussen et al. (Rasmussen et al., 2004) have already revealed intriguing differences between pigeon pectoralis mitochondria and the skeletal muscle of several mammals, patterns reported initially by the important and pioneering studies of Suarez et al. in hummingbirds (Suarez et al., 1991). Thus, we sought to extend these important seminal works to another avian species.

The primary muscles utilized during locomotion in each species were compared as these are the largest contributors to oxygen consumption during exercise. Mitochondria from rat quadriceps femoris and triceps surae muscle groups were contrasted with sparrow pectoralis, a flight muscle that accounts for ~15.5% of body mass and accounts for a large fraction of oxygen consumption during flight, as all flight muscles totalled account for 17% of total body mass (Schmidt-Nielsen, 1984). The locomotory muscles of the rat hindlimb used in the present study are over 90% type II, whereas sparrow pectoralis is 100% type II. Specifically, rat muscles used for mitochondrial isolation consisted of 71.7% fast glycolytic fibers (type IIb), with fast oxidative glycolytic (type IIa) and slow oxidative fibers (type I) constituting the remaining 20.5 and 7.8%, respectively (Armstrong and Phelps, 1984). Sparrow pectoralis is comprised exclusively of fast oxidative glycolytic fibers (George and Berger, 1966; Rosser and George, 1986).

Animal and muscle preparation

All procedures were in accordance with the guidelines regarding the care and use of animals by the Institutional Animal Care and Use Committee at Arizona State University. On the morning of each experiment, English sparrows [*Passer domesticus* (Linnaeus 1758)] weighing 22.5–26.5 g were captured at a livestock auction (Phoenix East Valley, AZ, USA) by mist net. Based on reported sparrow feeding patterns and the food availability at the collection site, their diet likely consisted of grain-based animal feeds and cereal grains with possible weeds, grass seeds and insects (Anderson, 2006). Rats were fed the Teklad Global 18% Protein Rodent Diet with 18.6% crude protein, 6.2% fat and 44.2% available carbohydrate (Harlan Laboratories, Indianapolis, IN, USA). As typical cow grain and protein feeds consist of 11.6–42.9% crude protein and 6.3–9.8% fat, the diet of these species, specifically in regards to fat content, likely did not differ dramatically (Hall et al., 2009). Sparrows were fasted 2–3 h prior to experiments to allow transport to the laboratory. After euthanization with an overdose of CO_2, the breast was plucked clean of feathers and the pectoralis muscle was extracted and removed from the keel. Sprague-Dawley rats [*Rattus norvegicus* (Berkenhout 1769)], weighing 250–350 g, were similarly administered a CO_2 overdose, hindquarters were quickly skinned, and the quadriceps femoris and triceps surae muscle groups were rapidly excised. Small samples (~0.5 g) of sparrow pectoralis and rat triceps surae were frozen in liquid nitrogen and stored at –80°C. The remaining excised muscles were immediately put in an ice-cold solution containing (in mmol l^{-1}) 100 KCl, 40 Tris HCl, 10 Tris base, 5 $MgCl_2$, 1 EDTA and 1 ATP, pH 7.4 (solution I) (Makinen and Lee, 1968).

Isolation of mitochondria

Mitochondrial isolations were performed at 0–4°C as described by Makinen and Lee (Makinen and Lee, 1968). Excised muscles were trimmed of fat and connective tissues and then minced, weighed and placed in nine volumes of solution I. Protease (Subtilisin A; Sigma-Aldrich, St Louis, MO, USA) was added (5 mg g^{-1} wet muscle), and the digested mince was mixed continually for 7 min. An equal volume of solution I was added to end digestion. The mince was homogenized with an Ultra-Turrax (Cincinnati, OH, USA) blender for 15 s at 40% of full power. The homogenate was then centrifuged at 700 ***g*** for 10 min in a refrigerated centrifuge (model J2-21M/E, Beckman, Fullerton, CA, USA) to pellet down contractile protein and cellular debris. The supernatant was rapidly decanted through a double layer of cheesecloth and centrifuged at 14,000 ***g*** for 10 min to pellet down the mitochondrial fraction. The supernatant was discarded and the mitochondrial pellet was resuspended and washed in a volume equal to the original homogenate in a solution containing (in mmol l^{-1}) 100 KCl, 40 Tris HCl, 10 Tris base, 1 $MgCl_2$, 0.1 EDTA, 0.2 ATP and 2% (w/v) bovine serum albumin (BSA) (no. A-7030, Sigma-Aldrich; fatty acid content <0.01%), pH 7.4 (solution II), and the suspension was centrifuged at 7000 ***g*** for 10 min. The supernatant was discarded, and the pellet was resuspended in a solution identical to solution II, but without BSA (solution III). This resuspended pellet was subsequently centrifuged at 3500 ***g*** for 10 min.

The final mitochondrial pellet was suspended in 400–600 µl of a solution containing (in mmol l^{-1}) 220 mannitol, 70 sucrose, 10 Tris HCl and 1 EGTA, pH 7.4, yielding a final protein content of 5.2–11.3 mg mitochondrial protein ml^{-1} for sparrows and 8.0–11.1 mg ml^{-1} for rats (Lowry et al., 1951).

Citrate synthase

Citrate synthase (CS) activity was assayed at 37°C as described by Srere (Srere, 1969) in both mitochondrial fractions and whole-muscle homogenates. Homogenates (10% w/v) were prepared by suspending ~0.1 g frozen muscle in nine volumes of ice-cold 10 mmol l^{-1} KPO_4, pH 7.5, in glass tubes followed by four to five complete passes with a motor-driven ground glass pestle. Mitochondrial suspension and homogenate aliquots were further diluted in 10 mmol l^{-1} KPO_4 and added to a cuvette containing 100 mmol l^{-1} Tris HCl, 0.1 mmol l^{-1} 5,5′-dithiobis-(2-nitrobenzoic acid) (DTNB), 0.25 mmol l^{-1} acetyl-CoA and 0.1% Triton. Substrate-dependent activity was initiated by addition of 0.5 mmol l^{-1} oxaloacetate into a final volume of 1.0 ml and absorbance was followed at 412 nm. Activity was calculated using a millimolar extinction coefficient of 13.6 for the mercaptide ion.

Mitochondrial content

Mitochondrial content of the whole muscle (mg mitochondrial protein g^{-1} wet muscle) was calculated as the CS activity of whole muscle homogenate (units g^{-1} wet muscle) divided by mitochondrial specific activity (units mg^{-1} mitochondrial protein).

Transmission electron microscopy and volume density

For transmission electron microscopy (TEM), one sparrow pectoralis muscle sample was excised immediately after euthanasia, cut into small pieces (~2×1×1 mm) and placed in 100 mmol l^{-1} cacodylate with 2.5% glutaraldehyde, pH 7.4, overnight at 4°C. The tissue was post-fixed for 1 h at room temperature in 100 mmol l^{-1} cacodylate with 1.0% osmium tetroxide, pH 7.4, and then stained in 0.25% uranyl acetate overnight at 4°C. Next, the sample was dehydrated in ethanol and embedded in epoxy resin, thin sectioned (70 nm) using

an RMC Ultra Microtome 6000 (Boeckeler, Tucson, AZ, USA) and placed on 200-mesh fomvar-coated copper grids. Finally, the sample was post-stained with uranyl acetate and lead citrate and imaged with a JEOL 400 EX transmission electron microscope (JEOL, Tokyo, Japan) with an accelerating voltage of 80 kV fitted with a SIA L3C digital camera (SIA, Duluth, GA, USA).

Mitochondrial volume density was estimated using classic stereological methods described by Weibel (Weibel, 1980). A grid consisting of evenly spaced points was laid onto electron micrographs of the intermyofibrillar portion of the muscle fiber (magnification ×15k) and the number of intersection points falling on mitochondria were divided by the total number of points falling in the micrograph area. Mitochondrial volume density was expressed as a percent.

State 3 (maximal) respiration and functional integrity of isolated mitochondria

Mitochondrial oxygen consumption rate ($\dot{J}_{O_2}$) was measured as described by Messer et al. (Messer et al., 2004). Briefly, $\dot{J}_{O_2}$ was measured polarographically in a respiration chamber (Rank Brothers, Cambridge, UK) maintained at 37°C. Incubations were carried out in a 2.0-ml final volume of respiration medium (RM) adapted from Wanders et al. (Wanders et al., 1984). The basic RM contained (in mmol l^{-1}) 100 KCl, 50 MOPS, 20 Glucose, 10 K_2PO_4, 10 $MgCl_2$, 1 EGTA and 0.2% BSA, pH 7.0.

Mitochondria, 100–200 μg protein, were added to 2.0 ml RM with P+M (1 mmol l^{-1} each) as oxidative substrates. State 3 $\dot{J}_{O_2}$ was initiated with a bolus addition of 1 μmol ADP. State 3 and state 4 (resting) $\dot{J}_{O_2}$, as described by Estabrook (Estabrook, 1967), were measured, and the respiratory control ratio (RCR) was calculated as the state 3:state 4 ratio. The ADP/O ratio (ADP phosphorylated per oxygen atom consumed) was also determined (Estabrook, 1967).

Substrates at saturating levels were selected for respiration and superoxide production measurements with the goal of providing reasonably physiologic fuel mixtures. Fatty acid was provided as PC+M (10 μmol l^{-1} + 1.0 mmol l^{-1}). Carbohydrate-related fuels were P+M (1.0 mmol l^{-1} + 1.0 mmol l^{-1}), glutamate + malate (G+M; 10 mmol l^{-1} + 1.0 mmol l^{-1}), P+G+M and the two cytosolic-mitochondrial electron shuttles. The glycerol 3-phosphate (G3P) shuttle was reconstructed by adding G3P (10 mmol l^{-1}) (Bremer and Davis, 1975). The mitochondrial steps of the malate–aspartate shuttle were reconstructed with glutamate + malate + arsenite (G+M+A; 10 mmol l^{-1} + 1.0 mmol l^{-1} + 2.0 mmol l^{-1}). Arsenite inhibits 2-oxoglutarate (2-OG) dehydrogenase, which precludes 2-OG oxidation and, further, impedes the thermodynamically unfavorable glutamate dehydrogenase reaction. Thus, glutamate metabolism is biased towards transamination with oxaloacetate forming aspartate. The electrogenic exchange of anionic aspartate for undissociated glutamic acid, driven by the membrane potential ($\Delta\Psi$), advances malate oxidation and NADH production at malate dehydrogenase.

Sensitivity of respiratory control

Intermediate steady-state $\dot{J}_{O_2}$ was established using a modification of the creatine kinase (CK) energetic clamp we have described previously (Lefort et al., 2010) to set energy phosphate levels in the incubation. Briefly, progressive changes in the ATP:ADP ratio were fixed by manipulating the phosphocreatine:creatine ratio (PCr:Cr). Incubations were primed with 5 mmol l^{-1} Cr, 5 mmol l^{-1} ATP and excess CK, and then stepwise PCr additions gave PCr:Cr ratios of 0.5, 1.0, 1.5, 2.0, 3.0 and 4.0 while $\dot{J}_{O_2}$ was followed continuously. The large total creatine pool prevents mitochondrial ATP production from causing any significant change in the ATP:ADP ratio. The inclusion of inorganic phosphate (P_i) at 10 mmol l^{-1} allowed the calculation of ΔG_{ATP}. Substrates provided were either P+M (1.0 mmol l^{-1} each) or PC+M (10 μmol l^{-1} + 1.0 mmol l^{-1}). For both fuel combinations, the sensitivity of respiratory control was assessed as K_MADP from Eadie–Hofstee plots and also as the slope of ΔG_{ATP}:$\dot{J}_{O_2}$ ('force–flow' relationship).

Net H_2O_2 release

Net hydrogen peroxide release by intact mitochondria was assessed as hydrogen peroxide (H_2O_2) accumulation using Amplex Red™ (AR) (Molecular Probes, Eugene, OR, USA) and horseradish peroxidase (HRP) (Muller et al., 2008). Briefly, mitochondria (0.1 mg mitochondrial protein ml^{-1}) were incubated in 200 μl RM at 37°C in the presence of 50 μmol l^{-1} AR and 0.1 U ml^{-1} HRP. Fuel combinations matched those for maximal $\dot{J}_{O_2}$ measurements, and oligomycin was included to inhibit ATP synthase and promote maximal H_2O_2 production. Assays were initiated by the addition of mitochondria, and fluorescence (excitation 550 nm, emission 590 nm) was followed for 30 min in a 96-well microplate reader (TECAN GENios, Durham, NC, USA). Standard curves, which included mitochondria to account for fluorescence quenching, were run daily and H_2O_2 release was expressed as pmol H_2O_2 min^{-1} mg^{-1} mitochondrial protein (St-Pierre et al., 2002). To approximate the rate of superoxide production, the net rate of H_2O_2 release can be multiplied by two.

ETC activities

Mitochondrial cytochrome *c* reductase activity was measured according to the methods of Gohil et al. (Gohil et al., 1981). Three different substrates were assessed, chosen for their various entry points into the ETC: 0.2 mmol l^{-1} NADH, 10 mmol l^{-1} succinate and 10 mmol l^{-1} G3P. Mitochondrial suspensions were diluted in 10 mmol l^{-1} kPO_4 (pH 7.5) and sonicated in two 10 s bursts with a Branson Sonifier at 40% full power. Sonicated mitochondria were added to a cuvette containing 200 μmol l^{-1} ADP, 200 μmol l^{-1} cyanide and 200 μmol l^{-1} oxidized cytochrome *c* (type VI, Sigma-Aldrich), and after substrate addition, the reduction of cytochrome *c* was followed at 550 nm. Activities were calculated using a millimolar extinction coefficient of 24.4 and are reported as nmol cytochrome *c* reduced mg^{-1} mitochondrial protein min^{-1}.

Statistics

Differences in enzyme activities, maximal and submaximal $\dot{J}_{O_2}$, H_2O_2 release and cytochrome *c* reductase activity between the species were analyzed using independent *t*-tests with significance set at $P<0.05$. Differences in maximal and submaximal $\dot{J}_{O_2}$, the slopes of the ΔG_{ATP}:$\dot{J}_{O_2}$ relationships and H_2O_2 release between different fuels within a species were analyzed using paired *t*-tests with significance set at $P<0.05$.

RESULTS

Citrate synthase

CS activities of whole muscle homogenate and mitochondrial preparations are shown in Table 1. Compared with rat, sparrow CS activity was eight times higher in skeletal muscle homogenate and 1.5 times higher in the mitochondrial pellet. Sparrow pectoralis homogenate CS activities were similar to avian values in the literature, which range from 200 to 450 μmol g^{-1} min^{-1} (Ardawi et al., 1989; Marsh, 1981; Marsh and Dawson, 1982; Suarez et al., 1986). Rat hindlimb muscle values were also representative of literature values (Baldwin et al., 1972; Willis et al., 1987).

Table 1. Muscle homogenate and mitochondrial citrate synthase activities in sparrow and rat

	Whole muscle homogenate (μmol g^{-1} min^{-1})	Mitochondria (μmol mg^{-1} min^{-1})	Mitochondrial density (mg g^{-1})
Sparrow pectoralis	380.6±37.1*	4.3±0.6*	94.3±11.6*
Rat mixed hindlimb	46.2±4.7	2.7±0.3	17.9±2.7

Mitochondrial density was calculated as homogenate citrate synthase (CS) activity divided by mitochondrial-specific CS activity.
Values are means ± s.e.m.; *N*=6 for both species.
*Significantly different from rat (*P*<0.05).

Mitochondrial content

The mitochondrial yield (mg mitochondrial protein g^{-1} wet mass) was 1.6±0.2 in sparrow pectoralis muscle and 1.2±0.1 in rat mixed hindlimb muscle. The calculated mitochondrial content based on CS activities in whole tissue homogenate and isolated mitochondria was over five times higher in sparrow pectoralis than rat mixed hindlimb muscle (94.3±11.6 and 17.9±2.7 mg g^{-1}, respectively; Table 1). Previous investigations have reported a mitochondrial content of 16–19 mg g^{-1} for rat mixed hindlimb and soleus (Davies et al., 1981; Rasmussen et al., 2004), 38.5 mg g^{-1} for pigeon pectoralis (Rasmussen et al., 2004) and 193 mg g^{-1} for hummingbird pectoralis (Suarez et al., 1991).

TEM and volume density

Electron micrographs of sparrow pectoralis muscle revealed large mitochondria with densely packed cristae in both subsarcolemmal and intermyofibrillar (IMF) regions of the muscle (Fig. 1). In the IMF sections, closely associated, elongated mitochondria can be seen located between myofibrils (Fig. 1B). The calculated IMF mitochondrial volume density in sparrow pectoralis was 25.4±3.3%, approximately five times higher than reported values for the extensively studied rat mixed hindlimb muscle (Esteva et al., 2008; Johnson et al., 1990; Philippi and Sillau, 1994). The determined sparrow pectoralis mitochondrial volume density corroborated a single study that determined English sparrow mitochondrial volume density to be 29.9%. This value is also comparable to reported values for the pigeon (30%), the eared grebe (32%) and the rufous hummingbird (33%) (Gaunt et al., 1990; James and Meek, 1979; Suarez et al., 1991).

State 3 respiration and functional integrity of isolated mitochondria

Table 2 presents the maximal oxidative capacities of isolated mitochondria in the presence of various substrates at saturating levels. ADP/O and RCR values for the various fuel combinations are also presented. P+M oxidative capacity was 510.1±30.3 nmol O_2 mg^{-1} min^{-1} for mitochondria isolated from sparrow pectoralis muscle and 640.3±95.1 for rat mixed hindlimb muscle and, like state 3 $\dot{J}_{O_2}$ for all substrates save PC+M and G3P, were not significantly different between species (Table 2). Mitochondria isolated from both species maintained high functional integrity, with P+M RCR values of 10.9±2.9 for sparrow and 8.6±0.8 for rat (Table 2). State 4 respiration rate, an indication of the degree of uncoupling in an isolated mitochondria preparation, did not differ between the species for any fuel examined (Table 2).

Notably, sparrow PC+M state 3 $\dot{J}_{O_2}$ was 1.9-fold higher than rat, and relative PC+M/P+M oxidation was over two times higher in sparrow than rat (0.76±0.07 *vs* 0.35±0.04, respectively; Fig. 2). Additionally, sparrow mitochondria showed an inability to oxidize G3P (Table 2). P+G+M elicited the highest state 3 $\dot{J}_{O_2}$ in both species. Interestingly, the mitochondrial steps of the malate–aspartate shuttle (the G+M+A substrate combination) supported state 3 respiration rates 65–70% of P+M in both species (Table 1).

Sensitivity of respiratory control

A near linear relationship between extramitochondrial ΔG_{ATP} and $\dot{J}_{O_2}$ was observed regardless of respiratory fuel, P+M or PC+M, or species (Fig. 3A,B). In rat mitochondria, the slope of the ΔG_{ATP}:$\dot{J}_{O_2}$

Table 2. Maximal oxidase activities (state 3 $\dot{J}_{O_2}$), coupling and respiratory control ratios (RCRs) in mitochondria from sparrow pectoralis and rat mixed hindlimb muscle

	Sparrow pectoralis				Rat mixed hindlimb			
Substrate	State 3 (nmol O_2 mg^{-1} min^{-1})	State 4 (nmol O_2 mg^{-1} min^{-1})	ADP/O	RCR	State 3 (nmol O_2 mg^{-1} min^{-1})	State 4 (nmol O_2 mg^{-1} min^{-1})	ADP/O	RCR
P+M	510.1± 30.3 (8)	60.2±8.2	2.68±0.15	10.9±2.9	640.3±95.1 (6)	76.6±10.3	2.56±0.11	8.6±0.8
G+M	608.9±36.8 (7)	66.6±12.3	2.69±0.08*	11.2±2.2	715.6±68.3 (6)	89.1±19.5	2.30±0.11	9.7±1.7
P+G+M	672.4±36.3 (7)	65.9±7.7	2.36±0.13	11.9±2.6	787.9±104.7 (6)	91.8±9.9	2.16±0.07	8.6±0.4
PC+M	395.2±36.6* (7)	78.5±10.8	2.65±0.11	5.5±0.7	211.9±20.6 (6)	80.9±17.5	2.24±0.18	3.8±0.6
G+M+A	330.1±26.0 (7)	72.1±8.6	2.16±0.06	4.8±0.4	452.9±36.9 (4)	84.6±5.9	2.19±0.19	5.4±0.2
G3P	10.6±1.5* (3)	n.d.	n.d.	n.d.	162.1±44.6 (3)	96.9±52.2	1.29±0.05	2.0±0.3

Values are means ± s.e.m. of the number of mitochondrial isolations shown in parentheses. RCR=state 3/state 4. Pyruvate (P)=1 mmol l^{-1}, malate (M)=1 mmol l^{-1}, glutamate (G)=10 mmol l^{-1}, palmitoyl-L-carnitine (PC)=10 μmol l^{-1}, succinate (Succ)=10 mmol l^{-1}, glycerol 3-phosphate (G3P)=10 mmol l^{-1} and arsenite (A)=2 mmol l^{-1}.
ADP/O, ADP phosphorylated per oxygen atom consumed; n.d., not determined.
*Significantly different from rat (*P*<0.05).

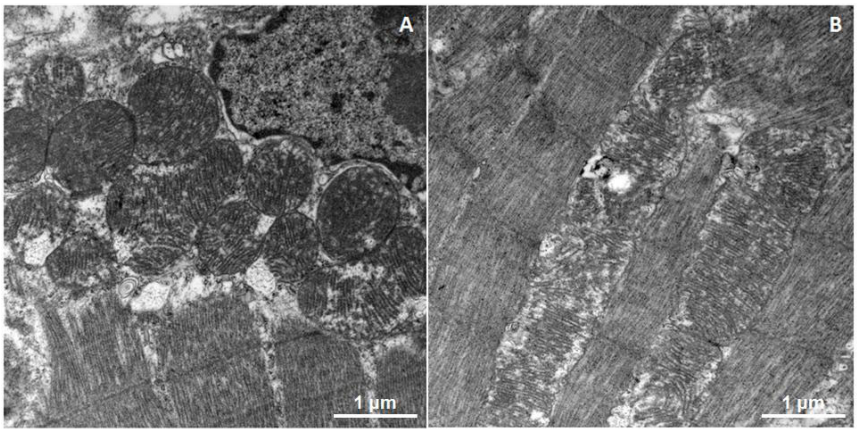

Fig. 1. Transmission electron micrographs (TEMs) of longitudinally sectioned sparrow pectoralis muscle. (A) Subsarcolemmal section showing a nucleus in the upper right corner bordering densely packed mitochondria. Fibers can be seen in the lower portion of the micrograph. (B) Intermyofibrillar section with large, highly reticulated mitochondria lying between adjacent fibers. TEM magnification, ×15k.

relationship with P+M is nearly three times greater than with PC+M, whereas in sparrow the slope is similar for these substrates. Additionally, the apparent K_MADP from Eadie–Hofstee plots for PC+M was significantly lower than that for P+M in rat mitochondria, a pattern also observed in human mitochondria (Sahlin et al., 2007). For any given preparation, the K_MADP for PC+M was less than that for P+M in sparrow mitochondria, though the effect failed to reach statistical significance (P=0.056). Apparent K_MADP was 50% higher in sparrow than rat mitochondria that were provided PC+M (Fig. 3D).

Mitochondrial-specific activities were multiplied by tissue mitochondrial content to estimate the O_2 consumption rate per gram wet tissue (Fig. 3C). The result reveals much higher oxidative capacity in the avian muscle, which reflects the much higher tissue mitochondrial content (Fig. 3C). In particular, the Eadie–Hofstee analysis predicts over a fivefold greater capacity for fatty acid oxidation in sparrow muscle than rat (28 *vs* 5 μmol O_2 mg^{-1} min^{-1}, respectively). Indeed, even with the carbohydrate fuel pyruvate, sparrow (P+M) oxidative capacity exceeded that of rat by over threefold (42 *vs* 13 μmol O_2 mg^{-1} min^{-1}, respectively).

Net H_2O_2 release

Overall, rat muscle mitochondria produced more than 1.5 times the H_2O_2 of sparrow for all fuels, though no direct comparison for a given fuel reached statistical significance (Fig. 4). The highest H_2O_2 release occurred in both species with the substrates of the malate–aspartate shuttle. In the rat, this shuttle generated over 60 times more H_2O_2 release than P+M; a 25-fold difference was observed in the sparrow. H_2O_2 release with G3P was significantly higher than P+M in rat mitochondria.

ETC activities

Substrate cytochrome *c* reductase activities are shown in Fig. 5. Respiratory chain oxidation of NADH was approximately twofold higher in sparrow than in rat (2390.1±288.1 *vs* 1256.6±235.0 nmol cytochrome *c* reduced mg^{-1} min^{-1}, respectively). Similarly, succinate cytochrome *c* reductase activity was roughly 1.8 times higher in the sparrow than rat mitochondria (Fig. 5). The cytosolic reducing equivalent carrier G3P elicited no measurable oxidation by sparrow pectoralis mitochondria.

DISCUSSION

The present study demonstrates that sparrow pectoralis mitochondria show a robust capacity to oxidize fatty acid as well as a higher maximal rate of NADH oxidation compared with rat hindlimb muscle mitochondria. Despite these differences, *in vitro* sparrow ROS production was similar to that of rat. A particularly noteworthy outcome was the extremely high ROS production by both avian and mammalian mitochondria when glycolytic electron shuttle substrates were provided. These intriguing results suggest that avian preference for lipid oxidation *in vivo* could result in less oxidative stress in birds compared with mammals, consistent with the longer life expectancies of birds.

Mitochondrial content and whole-muscle fuel oxidation

Two common measures of the content of mitochondria in myocytes are volume density (ml mitochondria g^{-1} muscle) and protein content (mg mitochondrial protein g^{-1} wet muscle). In this study, mitochondrial protein content was roughly fivefold higher in sparrow pectoralis than in rat mixed hindlimb muscle, calculated by the ratio of CS activities in whole tissue homogenate and isolated mitochondria. Our rat value, 18 mg g^{-1}, corroborates published data on cage-sedentary rat hindlimb muscle mitochondrial contents in the range of 12–20 mg g^{-1} (Davies et al., 1981; Rasmussen et al., 2004), whereas the sparrow value of 94 mg g^{-1} is intermediate between reported values in pigeon [39 mg g^{-1} (Rasmussen et al., 2004)] and hummingbird [193 mg g^{-1} (Suarez et al., 1991)]. This pattern for mitochondrial content in the birds, hummingbird>sparrow>pigeon, is opposite to the body masses of these species. Because the metabolic cost of flight and whole-body maximum aerobic capacity ($\dot{V}_{O2,max}$) scale hypometrically with body

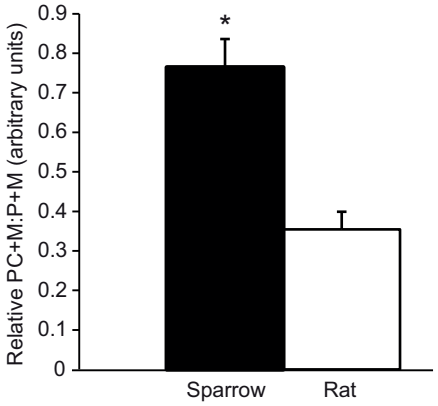

Fig. 2. Relative palmitoyl-L-carnitine + malate (PC+M):pyruvate + malate (P+M) ratio calculated by dividing the PC+M state 3 mitochondrial oxygen consumption rate ($\dot{J}_{O_2}$) by the P+M state 3 $\dot{J}_{O_2}$ of the same mitochondrial preparation. Values are means ± s.e.m.; N=5 sparrows and N=6 rats. *Significantly different from rat (P<0.05).

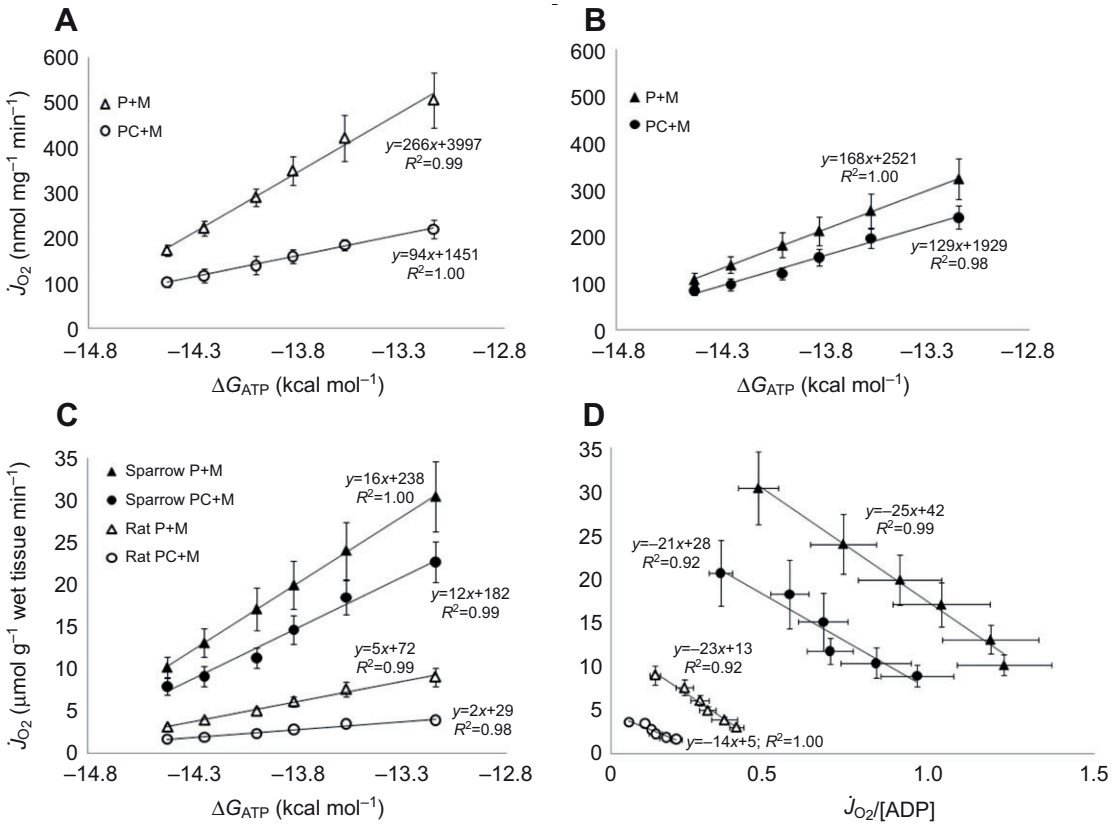

Fig. 3. Results of a progressive creatine kinase energetic clamp in rat mixed hindlimb and sparrow pectoralis mitochondria when provided either 1.0 mmol l^{-1} pyruvate + 1.0 mmol l^{-1} malate (P+M) or 10 μmol l^{-1} palmitoyl-L-carnitine + 1.0 mmol l^{-1} malate (PC+M). (A,B) Thermodynamic force–metabolic flow relationship between the free energy of ATP (ΔG_{ATP}) and oxygen consumption rate ($\dot{J}_{O_2}$) for rat (A) and sparrow (B) mitochondria. (C) Estimated whole-muscle O_2 consumption rate (μmol g^{-1} min^{-1}) as a function of ΔG_{ATP}, calculated by multiplying the mitochondrial $\dot{J}_{O_2}$ by tissue mitochondrial content. (D) Eadie–Hofstee plots of $\dot{J}_{O_2}$/[ADP] *vs* $\dot{J}_{O_2}$ (*N*=3–4). All data are means ± s.e.m.

mass (Schmidt-Nielsen, 1984), we explored the relationship between muscle mitochondrial protein content and mass-specific $\dot{V}_{O_2}$ during routine flight and maximal exercise.

Flight $\dot{V}_{O_2}$ and $\dot{V}_{O_2,max}$ values were calculated using well-known allometric relationships (Schmidt-Nielsen, 1984). Our rat mitochondrial content data were included in this analysis, along with published values for rat locomotion $\dot{V}_{O_2}$ and $\dot{V}_{O_2,max}$ (Brooks and Donovan, 1983). With mitochondrial protein content as the predictor variable, linear relations were observed for both locomotion $\dot{V}_{O_2}$ and $\dot{V}_{O_2,max}$ (Fig. 6). This finding, which supports the concept of symmorphosis, extends the pioneering work of Weibel et al. in two ways. First, Weibel et al. studied mammals only and showed a linear relationship between $\dot{V}_{O_2,max}$ and muscle mitochondrial content (assessed as volume density) across 11 species (Weibel et al., 2004; Weibel et al., 1991). The analysis considered here focuses mainly on avian species, but also includes the rat, a mammal extensively used in studies of exercise metabolism. Additionally, the predictor variable used by Weibel et al. was mitochondrial volume density, not protein content as used here. Our TEM data revealed sparrow pectoralis IMF mitochondrial volume density to be 25%, which is similar to pigeon and hummingbird pectoralis. Thus, if we were to substitute mitochondrial volume density as the predictor variable in Fig. 6, nearly vertical plots (i.e. no relationship at all) would result for the avian species. Two conclusions are suggested by this analysis. (1) It suggests that the previous relationship shown in mammals (Weibel et al., 2004; Weibel et al., 1991) would also be satisfactorily explained by muscle mitochondrial protein content. Indeed, in mammals, the protein:volume ratio appears to be relatively constant; standard 3-month rodent exercise training regimens have been shown to induce roughly twofold increases in rat muscle mitochondrial contents, measured either as protein content (mg g^{-1}) (Davies et al., 1981) or volume percent (Gollnick and King, 1969). Protein may therefore be the more important predictor. (2) Avian flight muscle

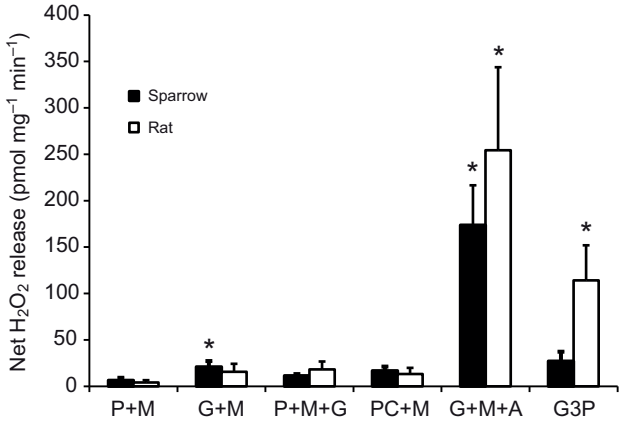

Fig. 4. Net H_2O_2 release by rat and sparrow mitochondria in the presence of oligomycin (static conditions). Substrates are defined as in Table 2. Values are means ± s.e.m.; *N*=4–6. *Significantly different from P+M (*P*<0.05).

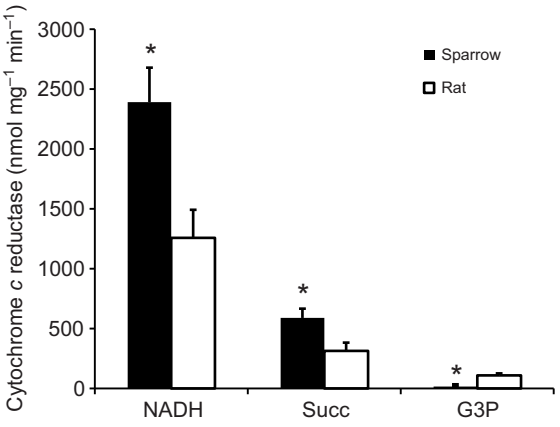

Fig. 5. Substrate cytochrome *c* reductase activities in sonicated mitochondria of sparrows and rats. Activity is expressed as nmol cytochrome *c* reduced mg^{-1} min^{-1}. Substrates were 0.15 mmol l^{-1} NADH, 10 mmol l^{-1} succinate (Succ) or 10 mmol l^{-1} G3P. Values are means ± s.e.m.; *N*=10 sparrows and *N*=7 rats. *Sgnificantly different from rat (*P*<0.05).

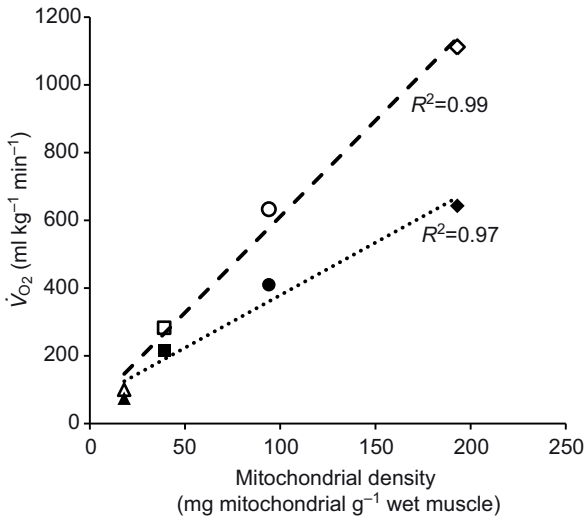

Fig. 6. Skeletal muscle mitochondrial density and $\dot{V}_{O_2}$. A linear relationship exists between mitochondrial density and both exercise $\dot{V}_{O_2}$ (closed symbols) and $\dot{V}_{O_2,max}$ (open symbols) in rat (triangles), pigeon (squares), sparrow (circles) and hummingbird (diamonds). Mitochondrial density data were obtained from the present study (rat and sparrow), Rasmussen et al. [pigeon (Rasmussen et al., 2004)] and Suarez et al. [hummingbird (Suarez et al., 1991)]. Bird exercise $\dot{V}_{O_2}$ was calculated as flight $\dot{V}_{O_2}=2.43M^{0.72}$ and $\dot{V}_{O_2,max}$ was calculated as $\dot{V}_{O_2,max}=2.90M^{0.65}$, from Schmidt-Nielson (Schmidt-Nielson, 1984), where *M* is body mass (kg). Rat $\dot{V}_{O_2}$ data were obtained from Brooks and Donovan (Brooks and Donovan, 1983) with exercise $\dot{V}_{O_2}$ corresponding to 75% $\dot{V}_{O_2,max}$. Pigeon, sparrow and hummingbird exercise $\dot{V}_{O_2}$ correspond to 76, 65 and 58% of $\dot{V}_{O_2,max}$, respectively.

mitochondria have apparently adapted to the extreme aerobic demand of flight by packing more catalytic machinery (metabolic protein) per unit of mitochondrial volume.

As Rome and Lindstedt have elegantly described, muscle cells must simultaneously meet the demands for force production (myofibrillar volume), cycling speed (sarcoplasmic reticulum volume) and endurance (mitochondrial volume) (Rome and Lindstedt, 1998). Taking this zero sum character of myocyte volume into account leads to the realization that mitochondrial volume expansion comes at the expense of myofibrillar and/or sarcoplasmic reticulum functional capacity. High-force-generating muscle (locomotory and cardiac myocytes) has an apparent limiting value for mitochondrial volume density, in the vicinity of 40%, an insight provided by Suarez et al. (Suarez et al., 1991) in their early studies in the hummingbird. Higher inner membrane surface area in avian flight muscle mitochondria may account for some of this additional protein density (Buser et al., 1982; Suarez et al., 1991). Data from trout are consistent with these observations: cold acclimatization causes an increase in mitochondrial protein content ($mg\,g^{-1}$) and cristae density without increasing volume density, which is already as high as 32% (St-Pierre et al., 1998). Indeed, we report high relative ETC activities in sparrow mitochondria, which corroborate previous data in the pigeon (Rasmussen et al., 2004).

Mitochondrial substrate oxidation

Complete carbohydrate combustion requires the oxidation of both pyruvate and cytosolic reducing equivalents, which are transferred into the mitochondria *via* either the NAD-linked malate–aspartate shuttle or the FAD-linked G3P shuttle (Fig. 8). The malate–aspartate shuttle dominates in oxidative tissues such as type I and cardiac muscle, whereas the G3P shuttle is important in type II muscle (Blanchaer, 1964; Digerness and Reddy, 1976; Jackman and Willis, 1996). To our knowledge this is the first study to report electron shuttle activities in avian mitochondria.

We measured the mitochondrial steps of the malate–aspartate shuttle with the substrate combination G+M+A and found similar state 3 $\dot{J}_{O_2}$ in sparrow and rat mitochondria (Table 2). Pyruvate oxidation rates were also similar, indicating comparable capacities for complete carbohydrate combustion. Notably, however, avian mitochondria lacked the ability to oxidize G3P. Thus, sparrow pectoralis muscle, which is composed exclusively of fast-twitch (type II) oxidative glycolytic fibers (George and Berger, 1966; Rosser and George, 1986), appears to exclusively transfer electrons *via* the malate–aspartate shuttle. This bias towards NAD-linked malate–aspartate shuttling would provide better energetic efficiency than the FAD-linked G3P shuttle when carbohydrate is the fuel. Thus, sparrow flight muscle mitochondria possess the capacity for high rates of complete carbohydrate combustion, comparable to that of rat hindlimb muscle.

Despite the similar rates of carbohydrate oxidation, there was a striking difference in the rate of fatty acid oxidation between the species. Palmitoyl-L-carnitine state 3 $\dot{J}_{O_2}$ was 1.9 fold faster in bird compared with rat mitochondria (Table 2). Thus, the ratio of PC+M:P+M (Fig. 3) is over 0.75 in sparrow, whereas it is less than 0.40 in rat. This pattern in sparrow *vs* rat is similar to the pattern in pigeon pectoralis compared with rat biceps reported previously by Rasmussen (Rasmussen et al., 2004), and in agreement with a (palmitoyl-CoA+carnitine+M):(P+M) ratio of 0.87 in hummingbird pectoralis mitochondria (Suarez et al., 1991).

Control of respiration

Although it is well established that mammalian muscle increasingly relies on carbohydrate at exercise intensities at or above the moderate range (Roberts et al., 1996) and that contractile failure ensues when carbohydrate is not available (Bergstrom and Hultman, 1967; Fitts et al., 1975; Messer et al., 2004), the scarce data on the fuel oxidation of flying birds indicate virtual complete reliance on fat oxidation at high fractions of $\dot{V}_{O_2,max}$ (Rothe, 1987; Suarez et

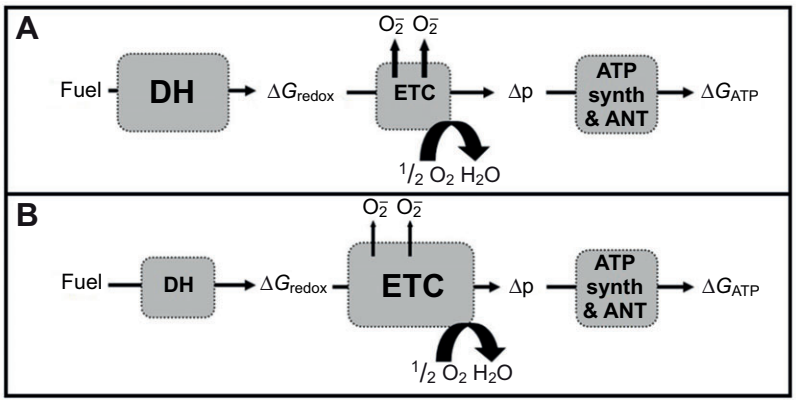

Fig. 7. Chemiosmotic energy transduction pathway (Mitchell, 1961). The first module represents substrate dehydrogenase enzymes (DH), the second module represents the electron transport chain (ETC) and the third module accounts for the combined actions of F_1-ATP synthase (ATP synth), the phosphate transporter and the adenine nucleotide translocase (ANT). As fuel is broken down, the chemical potential energy is transformed into a redox potential, or ΔG_{redox}. This energy is further transduced into the protonmotive force (Δp) *via* H^+ pumping as electrons travel down the ETC. The flux through any module is a function of the resistance to flow within that module and the driving force, or the disequilibrium between two energetic intermediates. Diagrams represent proposed mammalian (A) and avian (B) thermokinetic control.

al., 1991). In both sparrow and rat, lower K_MADP for respiration was observed with PC+M than P+M (Fig. 3D), a finding consistent with recent work by Sahlin et al. in human muscle (Sahlin et al., 2007). Lower PC+M K_MADP would provide a kinetic bias favoring fatty acid fuel selection when ADP concentrations are low, i.e. at low ATP turnover rates. This pattern is in agreement with the observation that humans predominantly rely on fat oxidation during walking at preferred speed (Willis et al., 2005).

Examining the effect of fuel on the thermodynamic force–metabolic flow relationship also elucidated further differences between the species (Fig. 3A–C). In contrast to mammals, the bird mitochondria in this study exhibited nearly identical ΔG_{ATP}:$\dot{J}_{O_2}$ relationships for P+M and PC+M, demonstrating that either pyruvate or fatty acid is equally competent to defend ATP free energy as ATP demand rises. Thus, bird mitochondria oxidizing solely fatty acid can match high ATP demand while defending a robust ATP free energy, which would minimize the inhibition of ATP utilizing processes (Jeneson et al., 2000).

Rat mitochondria, in contrast, must allow ΔG_{ATP} to fall to a much greater extent when fatty acid is the oxidized fuel, which is consistent with increasing reliance on carbohydrate as the energy demand increases and cellular energy state falls (Connett et al., 1985; Crowley et al., 1996). For example, rat mitochondria oxidizing P+M at a $\dot{J}_{O_2}$ of 220 nmol mg^{-1} min^{-1} defend ΔG_{ATP} at –14.2 kcal mol^{-1}, but if only PC+M is available then ΔG_{ATP} must fall to –13.3 kcal mol^{-1}. The much higher ADP, AMP and P_i associated with this fall in ATP energy would exert inhibitory influence on ATP-utilizing processes and an activation of glycolysis (Connett, 1988; Holloszy and Coyle, 1984; Jeneson et al., 2000; Saltin and Gollnick, 1983; Van der Meer et al., 1980). In the present study, fatty acid was provided as palmitoyl-L-carnitine, which enters the mitochondrial matrix downstream of carnitine palmitoyltransferase I (CPT1), a putative locus of control for lipid oxidation (Fig. 8A). Our findings corroborate others (Jackman and Willis, 1996; Willis and Jackman, 1994) showing fat cannot support high rates of oxygen consumption in rat muscle mitochondria even when CPT1 is entirely bypassed.

Electron transport chain

Sonicated sparrow mitochondria oxidized NADH and succinate over 1.8 times faster than rat, indicating a robust capacity for sparrow ETC electron transfer (Fig. 5), and corroborating previous data in the pigeon skeletal muscle (Rasmussen et al., 2004; Stevens, 1996) and sparrow liver mitochondria (Brown et al., 2009). However, consistent with our polarographic data, sparrow mitochondria showed no capacity to oxidize G3P. High avian ETC capacity to transfer electrons agrees with morphological data indicating higher surface density of the inner mitochondrial membrane in avian compared with mammalian muscle mitochondria (Hoppeler and Lindstedt, 1985). Specifically, in rat soleus, a cristae surface area of 27 m^2 per ml mitochondria volume has been reported compared with 57 m^2 per ml in hummingbird pectoralis (Buser et al., 1982; Suarez et al., 1991). The maximum flux by the complete oxidative pathway of P+M, in contrast, is similar in sparrow and rat mitochondria (Table 2). Taken together, these data reveal a large difference regarding the ability of matrix dehydrogenases to produce reducing equivalents compared with the capacity of the ETC to transfer them to O_2. For example, in rat, the ratio of the complete P+M pathway to that of NADH oxidation by the ETC (P+M:NADH) gives a value of 0.51. In the sparrow this ratio is only 0.21, indicating a much greater reserve capacity for electron flux down the ETC in the avian mitochondria. The same pattern was observed for P+G+M, with ratios of 0.63 in rat and 0.23 in sparrow. It is also intriguing to note that the PC+M:NADH ratio is identical (0.17) in both species.

Mitchell's chemiosmotic theory of oxidative phosphorylation (Mitchell, 1961) is shown schematically in Fig. 7. In sparrow muscle mitochondria, high ETC capacity relative to matrix dehydrogenases suggests that a lower redox potential is necessary to drive a given O_2 consumption rate (Fig. 7B), which may influence both fuel selection and ROS production. Lumeng et al. (Lumeng et al., 1976) showed in rat liver mitochondria oxidizing palmitoyl-L-carnitine that reconstitution of the malate–aspartate shuttle concomitantly reduced the matrix (the NADH:NAD ratio rose) as it abolished fatty acid oxidation. Moreover, this same suppression of fatty acid oxidation was observed when G3P was provided to liver mitochondria isolated from rats pretreated with thyroid hormone to upregulate the G3P shuttle, which does not ordinarily operate in the liver (Lee and Lardy, 1965). Human muscle exhibits a biphasic pattern of redox status as exercise intensity rises, with oxidation increasing with mild exercise followed by marked reduction as intensity exceeds the lactate threshold (Sahlin et al., 1987). We speculate that increased matrix reduction may account for both the suppressed fat oxidation and increased ROS production that have been observed in mammals exercising above the lactate threshold (Acevedo and Goldfarb, 1989; Achten and Jeukendrup, 2004). In birds, high ETC capacity may bias fuel selection towards fatty acids even during the high ATP demand of flight and thus may also minimize ROS production under these conditions.

Reactive oxygen species

Mitochondrial H_2O_2 release under oligomycin-inhibited (static) conditions was not statistically different between rat and sparrow

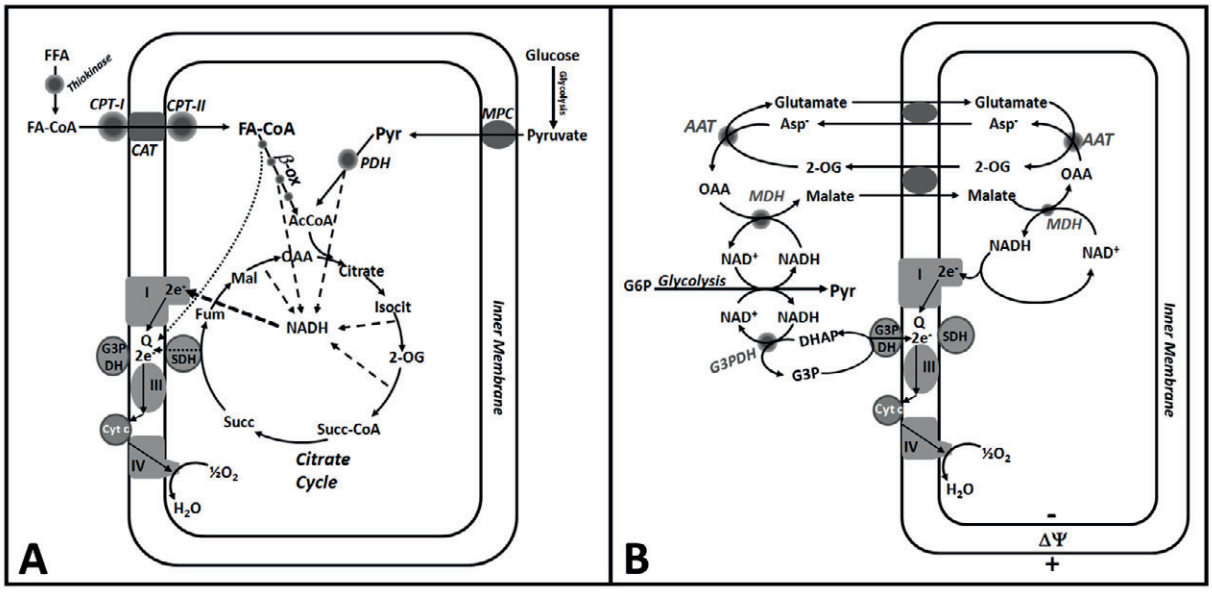

Fig. 8. Substrate oxidation and electron shuttle pathways. (A) Transportation and oxidation of fatty acids and glucose. Pyruvate moves into the matrix through the mitochondria pyruvate carrier (MPC) and yields 1 pair of NADH electrons and 1 acetyl-CoA (AcCoA) before entering the citric acid cycle. Fatty acyl-CoA (FA-CoA) is converted to a fatty acyl-carnitine *via* carnitine palmitoyltransferase I (CPT-I), enters the matrix through carnitine acylcarnitine translocase (CAT) and is converted back to a fatty acyl-CoA by CPT-II, which yields 1 NADH, 1 $FADH_2$ and 1 acetyl-CoA per β-oxidation (β-ox) cycle. The NADH-linked electrons gained from pyruvate dehydrogenase (PDH) and β-ox, along with those harvested in the dehydrogenase reactions of the citric acid cycle, enter the electron transport chain (ETC) at complex I and travel down the ETC until they ultimately reduce oxygen to water at complex IV. (B) Electron shuttle pathways. In the malate–aspartate shuttle, NADH electrons harvested during glycolysis are shuttled into the mitochondrial matrix by reducing oxaloacetate (OAA) to malate in the intermembrane space, exchanging malate for 2-oxogluterate (2-OG), and subsequently oxidizing malate in the matrix. The resultant matrix OAA then transaminates with matrix glutamate, forming aspartate (Asp), which is exchanged with intermembrane space glutamate. This allows for the regeneration of OAA and glutamate in the intermembrane space to permit the cycle to continue. In the glycerol-3-phosphate (G3P) shuttle, NADH electrons are donated to dihydroxyacetone phosphate (DHAP), producing G3P. These electrons can then enter the ETC at G3P dehydrogenase (G3P DH), reforming DHAP in the intermembrane space. AAT, aspartate aminotransferase; Cyt *c*, cytochrome *c*; FFA, free fatty acid; Fum, fumarate; G6P, glucose-6-phosphate; Mal, malate; MDH, malate dehydrogenase; Pyr, pyruvate; SDH, succinate dehydrogenase; Succ, succinate; succ-CoA, succinyl-CoA; ΔΨ, transmembrane electric potential difference.

muscle mitochondria. In fact, expressing the data per gram wet tissue using the experimentally determined tissue mitochondrial content predicts several-fold higher net H_2O_2 release in sparrow muscle. Previous investigations have produced varying results when comparing ROS production between birds and mammals (Barja, 1998; Barja and Herrero, 1998; Brown et al., 2009; Herrero and Barja, 1997; Herrero and Barja, 1998; Ku and Sohal, 1993). Rat and sparrow state 4 respiration rates (Table 2) indicate that the degree of uncoupling was similar between species and likely did not exert a differential effect on H_2O_2 production. Indeed, even if the degree of uncoupling was different between the species, proton leak pathways were not inhibited during the assay and thus the mitigating effects of uncoupling on ROS production were incorporated within the measurement.

A prominent outcome we observed was that mitochrondrial electron shuttle substrates, G+M+A in both rat and sparrow and G3P in the rat, resulted in order of magnitude higher ROS production than either P+M or PC+M, which has profound implications. Specifically, it is well known that high glucose availability to cells induces marked oxidative stress (Anderson et al., 2009; Brownlee, 2001), yet in general pyruvate is a very poor ROS substrate (Fig. 4) (Anderson and Neufer, 2006; St-Pierre et al., 2002). Our data support the concept that it is the electron shuttling requirement of aerobic glycolysis (Fig. 8), rather than the oxidation of pyruvate itself, that accounts for this. Indeed, although we could detect very little G3P oxidation by sparrow pectoralis mitochondria, significant H_2O_2 accumulation was nevertheless observed from this fuel, described previously as a 'high efficiency' generator of superoxide (Mracek et al., 2009). In mammalian mitochondria, ROS production rises with increasing protonmotive force and more negative redox potentials of electron carriers (Korshunov et al., 1997; St-Pierre et al., 2002), and an increase in matrix reduction is linked to a suppression of fat oxidation (Lumeng et al., 1976). If sparrow mitochondria are able to drive a given O_2 consumption rate with a lower redox potential, as suggested by the high ETC capacity relative to the matrix dehydrogenases, this may simultaneously result in a bias towards fat oxidation and an attenuation of ROS production in birds *in vivo*.

CONCLUSIONS

Mitochondria isolated from sparrow pectoralis muscle show a much higher maximal capacity to oxidize fatty acid than mitochondria from rat hindlimb muscle; however, the two types exhibit equal maximal capacities to oxidize carbohydrate-related substrates. ETC catalytic potential is much higher in sparrow, and this high ETC:oxidase ratio suggests that a lower redox potential is necessary to drive a given O_2 consumption rate in sparrow mitochondria. This decreased redox potential may result in less reliance on carbohydrate oxidation in birds and ultimately bring about lower ROS production *in vivo*.

LIST OF SYMBOLS AND ABBREVIATIONS

A	arsenite
$[ADP]_f$	cytosolic free ADP concentration
ANT	adenine nucleotide translocase

ATP synth	F_1-ATP synthase
CK	creatine kinase
CPT1	carnitine palmitoyltransferase I
Cr	creatine
CS	citrate synthase
DH	dehydrogenase enzyme
DTNB	5,5′-dithiobis-(2-nitrobenzoic acid)
ETC	electron transport chain
G	glutamate
G3P	glycerol-3-phosphate
HRP	horseradish peroxidase
IMF	intermyofibrillar
$\dot{J}_{O_2}$	rate of mitochondrial O_2 consumption
K_MADP	kinetic control of $\dot{M}_{O_2}$ by $[ADP]_f$ alone
M	malate
P	pyruvate
PC	palmitoyl-L-carnitine
PCr	phosphocreatine
P_i	inorganic phosphate
RCR	respiratory control ratio
RER	respiratory exchange ratio
RMR	resting metabolic rate
ROS	reactive oxygen species
RQ	respiratory quotient
$\dot{V}_{O_2,max}$	maximum rate of O_2 uptake
ΔG_{ATP}	free energy of ATP
ΔG_{redox}	redox potential
Δp	protonmotive force

ACKNOWLEDGEMENTS

The authors thank David Lowry for his help and guidance with electron microscopy sample preparation and imaging.

FUNDING

This research received no specific grant from any funding agency in the public, commercial or not-for-profit sectors.

REFERENCES

Acevedo, E. O. and Goldfarb, A. H. (1989). Increased training intensity effects on plasma lactate, ventilatory threshold, and endurance. *Med. Sci. Sports Exerc.* **21**, 563-568.

Achten, J. and Jeukendrup, A. E. (2004). Relation between plasma lactate concentration and fat oxidation rates over a wide range of exercise intensities. *Int. J. Sports Med.* **25**, 32-37.

Ahlborg, G., Felig, P., Hagenfeldt, L., Hendler, R. and Wahren, J. (1974). Substrate turnover during prolonged exercise in man. Splanchnic and leg metabolism of glucose, free fatty acids, and amino acids. *J. Clin. Invest.* **53**, 1080-1090.

Anderson, E. J. and Neufer, P. D. (2006). Type II skeletal myofibers possess unique properties that potentiate mitochondrial H_2O_2 generation. *Am. J. Physiol. Cell Physiol.* **290**, C844-C851.

Anderson, E. J., Kypson, A. P., Rodriguez, E., Anderson, C. A., Lehr, E. J. and Neufer, P. D. (2009). Substrate-specific derangements in mitochondrial metabolism and redox balance in the atrium of the type 2 diabetic human heart. *J. Am. Coll. Cardiol.* **54**, 1891-1898.

Anderson, T. R. (2006). *Biology of the Ubiquitous House Sparrow*. New York: Oxford University Press.

Ardawi, M. S., Majzoub, M. F., Masoud, I. M. and Newsholme, E. A. (1989). Enzymic and metabolic adaptations in the gastrocnemius, plantaris and soleus muscles of hypocaloric rats. *Biochem. J.* **261**, 219-225.

Armstrong, R. B. and Phelps, R. O. (1984). Muscle fiber type composition of the rat hindlimb. *Am. J. Anat.* **171**, 259-272.

Baldwin, K. M., Klinkerfuss, G. H., Terjung, R. L., Mole, P. A. and Holloszy, J. O. (1972). Respiratory capacity of white, red, and intermediate muscle: adaptative response to exercise. *Am. J. Physiol.* **222**, 373-378.

Baldwin, K. M., Reitman, J. S., Terjung, R. L., Winder, W. W. and Holloszy, J. O. (1973). Substrate depletion in different types of muscle and in liver during prolonged running. *Am. J. Physiol.* **225**, 1045-1050.

Barja, G. (1998). Mitochondrial free radical production and aging in mammals and birds. *Ann. N. Y. Acad. Sci.* **854**, 224-238.

Barja, G. and Herrero, A. (1998). Localization at complex I and mechanism of the higher free radical production of brain nonsynaptic mitochondria in the short-lived rat than in the longevous pigeon. *J. Bioenerg. Biomembr.* **30**, 235-243.

Barja, G., Cadenas, S., Rojas, C., Perez-Campo, R. and Lopez-Torres, M. (1994). Low mitochondrial free radical production per unit O_2 consumption can explain the simultaneous presence of high longevity and high aerobic metabolic rate in birds. *Free Radic. Res.* **21**, 317-327.

Belo, P. S., Romsos, D. R. and Leville, G. A. (1976). Blood metabolites and glucose metabolism in the fed and fasted chicken. *J. Nutr.* **106**, 1135-1143.

Bergman, B. C. and Brooks, G. A. (1999). Respiratory gas-exchange ratios during graded exercise in fed and fasted trained and untrained men. *J. Appl. Physiol.* **86**, 479-487.

Bergstrom, J. and Hultman, E. (1967). A study of the glycogen metabolism during exercise in man. *Scand. J. Clin. Lab. Invest.* **19**, 218-228.

Blanchaer, M. C. (1964). Respiration of mitochondria of red and white skeletal muscle. *Am. J. Physiol.* **206**, 1015-1020.

Bordel, R. and Haase, E. (1993). Effects of flight on blood parameters in homing pigeons. *J. Comp. Physiol. B* **163**, 219-224.

Bremer, J. and Davis, E. J. (1975). Studies on the active transfer of reducing equivalents into mitochondria via the malate-aspartate shuttle. *Biochim. Biophys. Acta* **376**, 387-397.

Brooks, G. A. and Donovan, C. M. (1983). Effect of endurance training on glucose kinetics during exercise. *Am. J. Physiol.* **244**, E505-E512.

Brooks, G. A. and Gaesser, G. A. (1980). End points of lactate and glucose metabolism after exhausting exercise. *J. Appl. Physiol.* **49**, 1057-1069.

Brown, J. C., McClelland, G. B., Faure, P. A., Klaiman, J. M. and Staples, J. F. (2009). Examining the mechanisms responsible for lower ROS release rates in liver mitochondria from the long-lived house sparrow (*Passer domesticus*) and big brown bat (*Eptesicus fuscus*) compared to the short-lived mouse (*Mus musculus*). *Mech. Ageing Dev.* **130**, 467-476.

Brownlee, M. (2001). Biochemistry and molecular cell biology of diabetic complications. *Nature* **414**, 813-820.

Burke, L. M., Hawley, J. A., Angus, D. J., Cox, G. R., Clark, S. A., Cummings, N. K., Desbrow, B. and Hargreaves, M. (2002). Adaptations to short-term high-fat diet persist during exercise despite high carbohydrate availability. *Med. Sci. Sports Exerc.* **34**, 83-91.

Buser, K. S., Kopp, B., Gehr, P., Weibel, E. R. and Hoppeler, H. (1982). Effect of cold environment on skeletal muscle mitochondria in growing rats. *Cell Tissue Res.* **225**, 427-436.

Calder, W. A. (1996). *Size, Function, and Life History*. New York: Dover.

Connett, R. J. (1988). Models of steady-state control of skeletal muscle VO_2 evaluation using tissue data. *Adv. Exp. Med. Biol.* **227**, 215-219.

Connett, R. J. and Honig, C. R. (1989). Regulation of VO_2 in red muscle: do current biochemical hypotheses fit in vivo data. *Am. J. Physiol.* **256**, R898-R906.

Connett, R. J., Gayeski, T. E. and Honig, C. R. (1985). Energy sources in fully aerobic rest-work transitions: a new role for glycolysis. *Am. J. Physiol.* **248**, H922-H929.

Coyle, E. F. (1995). Substrate utilization during exercise in active people. *Am. J. Clin. Nutr.* **61**, 968S-979S.

Crowley, M. A., Willis, W. T., Matt, K. S. and Donovan, C. M. (1996). A reduced lactate mass explains much of the glycogen sparing associated with training. *J. Appl. Physiol.* **81**, 362-367.

Davies, K. J., Packer, L. and Brooks, G. A. (1981). Biochemical adaptation of mitochondria, muscle, and whole-animal respiration to endurance training. *Arch. Biochem. Biophys.* **209**, 539-554.

Davis, E. and Davis-Van Thienen, W. (1989). Force–flow and back–pressure relationships in mitochondrial energy transduction: an examination of extended state 3–state 4 transitions. *Arch. Biochem. Biophys.* **275**, 449-458.

Digerness, S. B. and Reddy, W. J. (1976). The malate-aspartate shuttle in heart mitochondria. *J. Mol. Cell Cardiol.* **8**, 779-785.

Estabrook, R. (1967). Mitochondrial respiratory control and the polarographic measurement of ADP/O ratios. *Meth. Enzymol.* **10**, 41-47.

Esteva, S., Panisello, P., Casas, M., Torrella, J. R., Pages, T. and Viscor, G. (2008). Morphofunctional responses to anaemia in rat skeletal muscle. *J. Anat.* **212**, 836-844.

Fitts, R. H., Booth, F. W., Winder, W. W. and Holloszy, J. O. (1975). Skeletal muscle respiratory capacity, endurance, and glycogen utilization. *Am. J. Physiol.* **228**, 1029-1033.

Flatt, J. P. (1995). Use and storage of carbohydrate and fat. *Am. J. Clin. Nutr.* **61**, 952S-959S.

Gaunt, A. S., Hikida, R. S., Jehl, Jr, J. R. and Fenbert, L. (1990). Rapid atrophy and hypertrophy of an avian flight muscle. *Auk* **107**, 649-659.

Gee, G. F., Carpenter, J. W. and Hensler, G. L. (1981). Species differences in hematological values of captive cranes, geese, raptors, and quail. *J. Wildl. Manage.* **45**, 463-483.

George, J. C. and Berger, A. J. (1966). *Avian Myology*. New York: Academic Press.

Glancy, B., Barstow, T. and Willis, W. T. (2008). Linear relation between time constant of oxygen uptake kinetics, total creatine, and mitochondrial content in vitro. *Am. J. Physiol. Cell Physiol.* **294**, C79-C87.

Gohil, K., Jones, D. A. and Edwards, R. H. T. (1981). Analysis of muscle mitochondrial function with techniques applicable to needle biopsy samples. *Clin. Physiol.* **1**, 195-207.

Gollnick, P. D. and King, D. W. (1969). Effect of exercise and training on mitochondria of rat skeletal muscle. *Am. J. Physiol.* **216**, 1502-1509.

Gyulai, L., Roth, Z., Leigh, J. S., Jr and Chance, B. (1985). Bioenergetic studies of mitochondrial oxidative phosphorylation using ^{31}phosphorus NMR. *J. Biol. Chem.* **260**, 3947-3954.

Hall, J. B., Seay, W. W. and Baker, S. M. (2009). Nutrition and feeding of the cow-calf herd: essential nutrients, feed classification and nutrient content of feeds. Publication 400-011. Virginia Cooperative Extension.

Harman, D. (1956). Aging: a theory based on free radical and radiation chemistry. *J. Gerontol.* **11**, 298-300.

Helge, J. W., Watt, P. W., Richter, E. A., Rennie, M. J. and Kiens, B. (2001). Fat utilization during exercise: adaptation to a fat-rich diet increases utilization of plasma fatty acids and very low density lipoprotein-triacylglycerol in humans. *J. Physiol.* **537**, 1009-1020.

Herrero, A. and Barja, G. (1997). ADP-regulation of mitochondrial free radical production is different with complex I- or complex II-linked substrates: implications for

the exercise paradox and brain hypermetabolism. *J. Bioenerg. Biomembr.* **29**, 241-249.
Herrero, A. and Barja, G. (1998). H_2O_2 production of heart mitochondria and aging rate are slower in canaries and parakeets than in mice: sites of free radical generation and mechanisms involved. *Mech. Ageing Dev.* **103**, 133-146.
Holloszy, J. O. and Coyle, E. F. (1984). Adaptations of skeletal muscle to endurance exercise and their metabolic consequences. *J. Appl. Physiol.* **56**, 831-838.
Holmes, D. J. and Austad, S. N. (1995). The evolution of avian senescence patterns: implications for understanding primary aging processes. *Am. Zool.* **35**, 307-317.
Hoppeler, H. and Lindstedt, S. L. (1985). Malleability of skeletal muscle in overcoming limitations: structural elements. *J. Exp. Biol.* **115**, 355-364.
Hurley, B. F., Nemeth, P. M., Martin, W. H., 3rd, Hagberg, J. M., Dalsky, G. P. and Holloszy, J. O. (1986). Muscle triglyceride utilization during exercise: effect of training. *J. Appl. Physiol.* **60**, 562-567.
Jackman, M. R. and Willis, W. T. (1996). Characteristics of mitochondria isolated from type I and type IIb skeletal muscle. *Am. J. Physiol.* **270**, C673-C678.
James, N. T. and Meek, G. A. (1979). Stereological analyses of the structure of mitochondria in pigeon skeletal muscle. *Cell Tissue Res.* **202**, 493-503.
Jeneson, J. A., Westerhoff, H. V., Brown, T. R., Van Echteld, C. J. and Berger, R. (1995). Quasi-linear relationship between Gibbs free energy of ATP hydrolysis and power output in human forearm muscle. *Am. J. Physiol.* **268**, C1474-C1484.
Jeneson, J. A., Westerhoff, H. V. and Kushmerick, M. J. (2000). A metabolic control analysis of kinetic controls in ATP free energy metabolism in contracting skeletal muscle. *Am. J. Physiol. Cell Physiol.* **279**, C813-C832.
Jenni, L. and Jennie-Eiermann, S. (1998). Fuel supply and metabolic constraints in migrating birds. *J. Avian Biol.* **29**, 521-528.
Johnson, J. A., Willis, W. T., Dallman, P. R. and Brooks, G. A. (1990). Muscle mitochondrial ultrastructure in exercise-trained iron-deficient rats. *J. Appl. Physiol.* **68**, 113-118.
Korshunov, S. S., Skulachev, V. P. and Starkov, A. A. (1997). High protonic potential actuates a mechanism of production of reactive oxygen species in mitochondria. *FEBS Lett.* **416**, 15-18.
Ku, H. H. and Sohal, R. S. (1993). Comparison of mitochondrial pro-oxidant generation and anti-oxidant defenses between rat and pigeon: possible basis of variation in longevity and metabolic potential. *Mech. Ageing Dev.* **72**, 67-76.
Kushmerick, M. J., Meyer, R. A. and Brown, T. R. (1992). Regulation of oxygen consumption in fast- and slow-twitch muscle. *Am. J. Physiol.* **263**, C598-C606.
Lee, Y. P. and Lardy, H. A. (1965). Influence of thyroid hormones on L-alpha-glycerophosphate dehydrogenases and other dehydrogenases in various organs of the rat. *J. Biol. Chem.* **240**, 1427-1436.
Lefort, N., Glancy, B., Bowen, B., Willis, W. T., Bailowitz, Z., De Filippis, E. A., Brophy, C., Meyer, C., Hojlund, K., Yi, Z. et al. (2010). Increased reactive oxygen species production and lower abundance of complex I subunits and carnitine palmitoyltransferase 1B protein despite normal mitochondrial respiration in insulin-resistant human skeletal muscle. *Diabetes* **59**, 2444-2452.
Lowry, O., Rosebrough, J., Farr, A. and Randall, R. (1951). Protein measurement with the Folin Phenol reagent. *J. Biol. Chem.* **193**, 265-275.
Lumeng, L., Bremer, J. and Davis, E. J. (1976). Suppression of the mitochondrial oxidation of (-)-palmitylcarnitine by the malate-aspartate and alpha-glycerophosphate shuttles. *J. Biol. Chem.* **251**, 277-284.
Makinen, M. W. and Lee, C. P. (1968). Biochemical studies of skeletal muscle mitochondria. I. Microanalysis of cytochrome content, oxidative and phosphorylative activities of mammalian skeletal muscle mitochondria. *Arch. Biochem. Biophys.* **126**, 75-82.
Marsh, R. L. (1981). Catabolic enzyme activities in relation to premigratory fattening and muscle hypertrophy in the gray catbird (*Dumetella carlinensis*). *J. Comp. Physiol. B* **141**, 417-423.
Marsh, R. L. and Dawson, W. R. (1982). Substrate metabolism in seasonally acclimatized American goldfinches. *Am. J. Physiol. Regul. Integr. Comp. Physiol.* **242**, R563-R569.
Masoro, E. J. (1992). Retardation of aging processes by food restriction: an experimental tool. *Am. J. Clin. Nutr.* **55**, 1250S-1252S.
McCarter, R., Masoro, E. J. and Yu, B. P. (1985). Does food restriction retard aging by reducing the metabolic rate? *Am. J. Physiol. Endocrinol. Metab.* **248**, E488-E490.
McCarter, R. J. and McGee, J. R. (1989). Transient reduction of metabolic rate by food restriction. *Am. J. Physiol. Endocrinol. Metab.* **257**, E175-E179.
Messer, J. I., Jackman, M. R. and Willis, W. T. (2004). Pyruvate and citric acid cycle carbon requirements in isolated skeletal muscle mitochondria. *Am. J. Physiol. Cell Physiol.* **286**, C565-C572.
Mitchell, P. (1961). Coupling of phosphorylation to electron and hydrogen transfer by a chemi-osmotic type of mechanism. *Nature* **191**, 144-148.
Mracek, T., Pecinova, A., Vrbacky, M., Drahota, Z. and Houstek, J. (2009). High efficiency of ROS production by glycerophosphate dehydrogenase in mammalian mitochondria. *Arch. Biochem. Biophys.* **481**, 30-36.
Muller, F. L., Liu, Y., Abdul-Ghani, M. A., Lustgarten, M. S., Bhattacharya, A., Jang, Y. C. and Van Remmen, H. (2008). High rates of superoxide production in skeletal-muscle mitochondria respiring on both complex I- and complex II-linked substrates. *Biochem. J.* **409**, 491-499.
O'Brien, M. J., Viguie, C. A., Mazzeo, R. S. and Brooks, G. A. (1993). Carbohydrate dependence during marathon running. *Med. Sci. Sports Exerc.* **25**, 1009-1017.
Pearl, R. (1928). *The Rate of Living*. London: University of London Press.
Perez-Campo, R., Lopez-Torres, M., Rojas, C., Cadenas, S. and Barja, G. (1993). A comparative study of free radicals in vertebrates – I. Antioxidant enzymes. *Comp. Biochem. Physiol.* **105B**, 749-755.
Philippi, M. and Sillau, A. H. (1994). Oxidative capacity distribution in skeletal muscle fibers of the rat. *J. Exp. Biol.* **189**, 1-11.
Rasmussen, U. F., Vielwerth, S. E. and Rasmussen, H. N. (2004). Skeletal muscle bioenergetics: a comparative study of mitochondria isolated from pigeon pectoralis, rat soleus, rat biceps brachii, pig biceps femoris and human quadriceps. *Comp. Biochem. Physiol.* **137A**, 435-446.
Roberts, T. J., Weber, J. M., Hoppeler, H., Weibel, E. R. and Taylor, C. R. (1996). Design of the oxygen and substrate pathways. II. Defining the upper limits of carbohydrate and fat oxidation. *J. Exp. Biol.* **199**, 1651-1658.
Rome, L. C. and Lindstedt, S. L. (1998). The quest for speed: muscles built for high-frequency contractions. *News Physiol. Sci.* **13**, 261-268.
Rosser, B. and George, J. C. (1986). The avian pectoralis: histochemical characterization and distribution of muscle fiber types. *Can. J. Zool.* **64**, 1174-1185.
Rothe, H. J., Biesel W. and Nachtigall, W. (1987). Pigeon flight in wind tunnel. *J. Comp. Physiol. B* **157**, 99-109.
Rottenberg, H. (1973). The thermodynamic description of enzyme-catalyzed reactions. The linear relation between the reaction rate and the affinity. *Biophys. J.* **13**, 503-511.
Sahlin, K., Katz, A. and Henriksson, J. (1987). Redox state and lactate accumulation in human skeletal muscle during dynamic exercise. *Biochem. J.* **245**, 551-556.
Sahlin, K., Mogensen, M., Bagger, M., Fernstrom, M. and Pedersen, P. K. (2007). The potential for mitochondrial fat oxidation in human skeletal muscle influences whole body fat oxidation during low-intensity exercise. *Am. J. Physiol. Endocrinol. Metab.* **292**, E223-E230.
Saltin, B. and Gollnick, P. (1983). Skeletal muscle adaptability: significance for metabolism and performance. In *Handbook of Physiology,* Vol. 10 (ed. L. D. Peachy, R. H. Adrian and S. R. Geiger), pp. 555-631, Bethesda, MD: American Physiological Society.
Schmidt-Nielsen, K. (1984). *Scaling: Why is Animal Size So Important?* Cambridge: Cambridge University Press.
Schwilch, R., Jenni, L. and Jenni-Eiermann, S. (1996). Metabolic responses of homing pigeons to flight and subsequent recovery. *J. Comp. Physiol. B* **157**, 99-109.
Sohal, R. S., Ku, H. H., Agarwal, S., Forster, M. J. and Lal, H. (1994). Oxidative damage, mitochondrial oxidant generation and antioxidant defenses during aging and in response to food restriction in the mouse. *Mech. Ageing Dev.* **74**, 121-133.
Srere, P. (1969). Citrate synthase. *Methods Enzymol.* **13**, 3-5.
St-Pierre, J., Charest, P. M. and Guderley, H. (1998). Relative contribution of quantitative and qualitative changes in mitochondria to metabolic compensation during seasonal acclimatisation of rainbow trout *Oncorhynchus mykiss*. *J. Exp. Biol.* **201**, 2961-2970.
St-Pierre, J., Buckingham, J. A., Roebuck, S. J. and Brand, M. D. (2002). Topology of superoxide production from different sites in the mitochondrial electron transport chain. *J. Biol. Chem.* **277**, 44784-44790.
Starkov, A. A. and Fiskum, G. (2003). Regulation of brain mitochondrial H_2O_2 production by membrane potential and NAD(P)H redox state. *J. Neurochem.* **86**, 1101-1107.
Stevens, L. (1996). *Avian Biochemistry and Molecular Biology*. Cambridge: Cambridge University Press.
Suarez, R. K., Brown, G. S. and Hochachka, P. W. (1986). Metabolic sources of energy for hummingbird flight. *Am. J. Physiol. Regul. Integr. Comp. Physiol.* **251**, R537-R542.
Suarez, R. K., Lighton, J. R., Moyes, C. D., Brown, G. S., Gass, C. L. and Hochachka, P. W. (1990). Fuel selection in rufous hummingbirds: ecological implications of metabolic biochemistry. *Proc. Natl. Acad. Sci. USA* **87**, 9207-9210.
Suarez, R. K., Lighton, J. R., Brown, G. S. and Mathieu-Costello, O. (1991). Mitochondrial respiration in hummingbird flight muscles. *Proc. Natl. Acad. Sci. USA* **88**, 4870-4873.
Sweazea, K. L. and Braun, E. J. (2005). Glucose transport by English sparrow (*Passer domesticus*) skeletal muscle: have we been chirping up the wrong tree? *J. Exp. Zool. A* **303**, 143-153.
Sweazea, K. L. and Braun, E. J. (2006). Oleic acid uptake by in vitro English sparrow skeletal muscle. *J. Exp. Zool. A* **305**, 268-276.
Van der Meer, R., Westeroff, H. V. and Van Dam, K. (1980). Linear relation between rate and thermodynamic force in enzyme-catalyzed reactions. *Biochim. Biophys. Acta* **591**, 488-493.
Waddington, D. C. and Cockrem, J. F. (1987). Homing ability of the house sparrow. *Notornis* **34**, 57-58.
Wahren, J., Felig, P., Ahlborg, G. and Jorfeldt, L. (1971). Glucose metabolism during leg exercise in man. *J. Clin. Invest.* **50**, 2715-2725.
Wanders, R. J., Groen, A. K., Van Roermund, C. W. and Tager, J. M. (1984). Factors determining the relative contribution of the adenine-nucleotide translocator and the ADP-regenerating system to the control of oxidative phosphorylation in isolated rat-liver mitochondria. *Eur. J. Biochem.* **142**, 417-424.
Weibel, E. R. (1980). *Stereological Methods*. London, New York: Academic Press.
Weibel, E. R., Taylor, C. R. and Hoppeler, H. (1991). The concept of symmorphosis: a testable hypothesis of structure–function relationship. *Proc. Natl. Acad. Sci. USA* **88**, 10357-10361.
Weibel, E. R., Bacigalupe, L. D., Schmitt, B. and Hoppeler, H. (2004). Allometric scaling of maximal metabolic rate in mammals: muscle aerobic capacity as determinant factor. *Respir. Physiol. Neurobiol.* **140**, 115-132.
Willis, W. T. and Jackman, M. R. (1994). Mitochondrial function during heavy exercise. *Med. Sci. Sports Exerc.* **26**, 1347-1353.
Willis, W. T., Brooks, G. A., Henderson, S. A. and Dallman, P. R. (1987). Effects of iron deficiency and training on mitochondrial enzymes in skeletal muscle. *J. Appl. Physiol.* **62**, 2442-2446.
Willis, W. T., Ganley, K. J. and Herman, R. M. (2005). Fuel oxidation during human walking. *Metabolism* **54**, 793-799.